

Room-Temperature Electrically Injected AlGaIn-Based near-Ultraviolet Laser Grown on Si

Meixin Feng,^{†,‡,§} Zengcheng Li,^{†,‡} Jin Wang,^{†,§} Rui Zhou,^{†,||} Qian Sun,^{*,†,||} Xiaojuan Sun,[⊥] Dabing Li,[⊥] Hongwei Gao,[†] Yu Zhou,[†] Shuming Zhang,^{†,||} Deyao Li,[†] Liqun Zhang,[†] Jianping Liu,^{†,||} Huaibing Wang,[†] Masao Ikeda,[†] Xinhe Zheng,[§] and Hui Yang^{†,||}

[†]Key Laboratory of Nano-devices and Applications, Suzhou Institute of Nano-Tech and Nano-Bionics, Chinese Academy of Sciences (CAS), Suzhou 215123, China

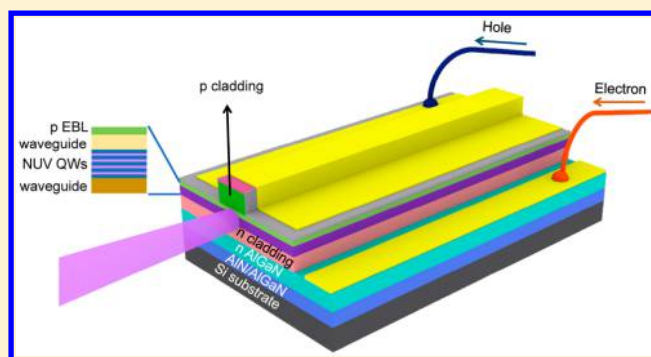
[§]University of Science and Technology Beijing, Beijing 100083, China

^{||}School of Nano Technology and Nano Bionics, University of Science and Technology of China, Hefei 230026, China

[⊥]State Key Laboratory of Luminescence and Applications, Changchun Institute of Optics Fine Mechanics and Physics, CAS, Changchun 130033, China

Supporting Information

ABSTRACT: This letter reports a successful fabrication of room-temperature electrically injected AlGaIn-based near-ultraviolet laser diode grown on Si. An Al-composition step down-graded AlN/AlGaIn multilayer buffer was carefully engineered to not only tackle the huge difference in the coefficient of thermal expansion between AlGaIn template and Si substrate, but also reduce the threading dislocation density caused by the large lattice mismatch. On top of the crack-free n-AlGaIn template, high quality InGaIn/AlGaIn quantum wells were grown, sandwiched by waveguide and optical cladding layers, for the fabrication of edge-emitting laser diode. A dramatic narrowing of the electroluminescence spectral linewidth, an elongated far-field pattern, and a clear discontinuity in the slope of light output power plotted as a function of the



injection current provide an unambiguous evidence of lasing.

KEYWORDS: AlGaIn, near-ultraviolet, laser, Si substrate, stress, defect

AlGaIn-based ultraviolet laser diodes (UV-LDs) have attracted intense research interest in the past few years due to their great potential application in laser microscopy, fluorescence spectroscopy, mass spectrometry, surface analysis, material processing, and laser lithography,^{1–4} and they may provide alternative solutions to conventional gas and solid-state UV lasers, which are large, heavy, inefficient, and inflexible in emission wavelength.

Today most of the AlGaIn-based UV-LDs are epitaxially grown on sapphire,^{1,3,4} costly free-standing GaN substrates^{2,5} or expensive small-size bulk AlN substrates.⁶ Compared with these substrates, Si substrates have a few advantages in wafer size, and material cost, as well as the depreciated automation processing line. By replacing these small-size expensive substrates with large-diameter cost-effective Si substrates, the cost of AlGaIn-based UV-LDs can be cut down to the level of light-emitting diode cost, which will further promote their applications. Furthermore, AlGaIn-based UV-LDs grown on Si may also serve as an on-chip light source for UV photonics integration.

Several other research groups attempted to grow III-nitride materials on Si and only achieved optically pumped lasing.^{7–10} Recently, we demonstrated room-temperature electrically

injected InGaIn-based visible LDs grown on Si.^{11,12} But the realization of AlGaIn-based near UV (NUV) LDs grown on Si is actually much more challenging than that of InGaIn-based visible LDs on Si. As the emission energy of NUV-LDs approaches the band gap of GaN, InGaIn NUV quantum wells (QWs) contain a very limited amount of indium with weakened localization states. Compared with visible QWs, the internal quantum efficiency (IQE) of NUV QWs is much more sensitive to the threading dislocation density (TDD).^{13,14} However, direct growth of AlGaIn on Si substrate encounters a very high TDD because of the large lattice mismatch.

Furthermore, a huge misfit in coefficient of thermal expansion (CTE) between AlGaIn and Si substrate usually induces a large tensile stress in the epitaxial film, and hence limits the maximum thickness of crack-free epitaxial film directly grown on Si. To reduce the threshold current of UV-LDs, AlGaIn-based optical cladding layers (CLs) with a relatively high Al content (~10%) are usually utilized to enhance the optical confinement of the active region.^{3,5} To

Received: October 15, 2017

Published: January 18, 2018

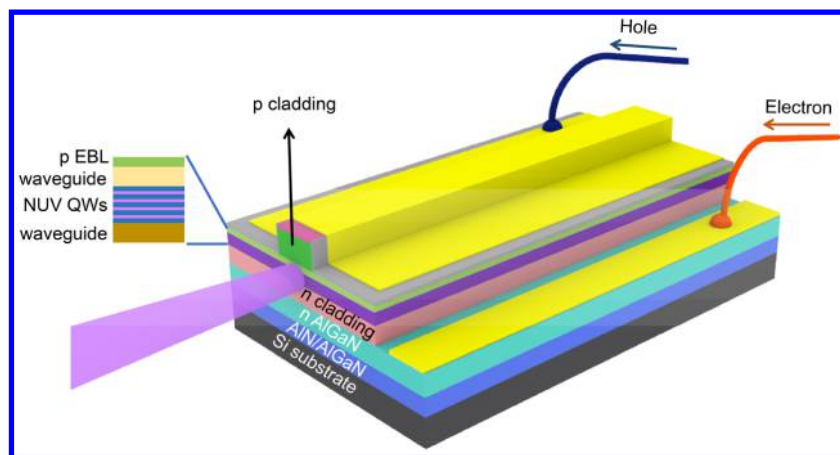


Figure 1. Schematic architecture of AlGaIn-based NUV-LD directly grown on Si.

avoid the formation of microcracks, AlGaIn template is often used to replace conventional GaN template and, hence, reduce the tensile stress in the thick AlGaIn optical CLs.^{2,15} The thick AlGaIn-based optical CLs and the GaN-based waveguide layers, together with the QWs and contact layers, often add up to a total thickness of 6–7 μm . However, it is quite challenging to grow crack-free high-quality AlGaIn-containing 6–7 μm thick film on Si substrate. Additionally, the crystalline quality of AlGaIn deteriorates with Al composition, owing to the small migration length of Al adatoms and their strong parasitic gas phase reaction with ammonia.^{16,17}

In this study, an Al-composition step down-graded AlN/AlGaIn multilayer buffer was carefully engineered to tackle the lattice mismatch and the CTE misfit for the epitaxial growth of high-quality Si-doped n-type AlGaIn thick template on Si substrate. On top of the AlGaIn template, an AlGaIn-based NUV laser structure was grown. After device fabrication, electrically injected AlGaIn-based NUV laser diode grown on Si was realized at room temperature for the first time.

The NUV laser structure was grown on Si (111) substrates using a metal–organic chemical vapor deposition (MOCVD) system. And it consisted of an unintentionally doped AlN/AlGaIn multilayer buffer, a 3.5 μm thick Si-doped n-type $\text{Al}_{0.03}\text{Ga}_{0.97}\text{N}$ thick layer with a doping level of $5 \times 10^{18} \text{ cm}^{-3}$, 150 pairs of 2.5 nm thick n-type $\text{Al}_{0.2}\text{Ga}_{0.8}\text{N}$ and 2.5 nm thick n-type GaN superlattice (SL) CLs, a 80 nm thick n-type GaN lower waveguide layer, four pairs of 2.5 nm thick undoped $\text{In}_{0.05}\text{Ga}_{0.95}\text{N}$ QWs and 10 nm thick undoped $\text{Al}_{0.1}\text{Ga}_{0.9}\text{N}$ quantum barrier layers, a 60 nm thick undoped GaN upper waveguide layer, a 20 nm thick p-type $\text{Al}_{0.25}\text{Ga}_{0.75}\text{N}$ electron blocking layer (EBL), 100 pairs of 2.5 nm thick p-type $\text{Al}_{0.2}\text{Ga}_{0.8}\text{N}$ and 2.5 nm thick p-type GaN SL CLs, and a 30 nm thick p-type GaN contact layer. The device was fabricated in a coplanar structure, with both p- and n-contact pads at the same side, as shown in Figure 1.

The unintentionally doped AlN/AlGaIn multilayer buffer consisted of a 300 nm thick AlN nucleation layer, a 420 nm thick $\text{Al}_{0.35}\text{Ga}_{0.65}\text{N}$ layer, and a 450 nm thick $\text{Al}_{0.17}\text{Ga}_{0.83}\text{N}$ layer. By using this multilayer buffer as a “hand-shaking” layer between $\text{Al}_{0.03}\text{Ga}_{0.97}\text{N}$ and Si substrate, a compressive strain was built up not only to compensate for the tensile stress due to the CTE mismatch during cooling down, but also facilitate the inclination, interaction, and even annihilation of TDs with each other.^{11,18–20} As shown in Figure 2a,b, a large amount of TDs

were annihilated at the interface, and the crystalline quality of $\text{Al}_{0.03}\text{Ga}_{0.97}\text{N}$ template was greatly improved.

On top of the high-quality $\text{Al}_{0.03}\text{Ga}_{0.97}\text{N}$ template grown on Si, the NUV laser structure was grown (Figure 2c). By optimizing the growth conditions, sharp interfaces of the InGaIn/AlGaIn QW active region were obtained (Figure 2d). The crystalline quality of the as-grown AlGaIn-based NUV laser wafer was evaluated by double-crystal X-ray rocking curve (DCXRC) measurements in a skew symmetric geometry. Figure 3a shows the typical rocking curves around the (0002) and (10 $\bar{1}$ 2) planes of the $\text{Al}_{0.03}\text{Ga}_{0.97}\text{N}$ template with a full width at half-maximum (fwhm) of 379 and 322 arcsec, respectively. From the measured XRC fwhm’s, the TDD in the $\text{Al}_{0.03}\text{Ga}_{0.97}\text{N}$ template was estimated to be around $6 \times 10^8 \text{ cm}^{-2}$. It should be pointed out that the DCXRC fwhm of the $\text{Al}_{0.03}\text{Ga}_{0.97}\text{N}$ (10 $\bar{1}$ 2) diffraction was even smaller than that of the $\text{Al}_{0.03}\text{Ga}_{0.97}\text{N}$ (0002) diffraction. And the edge-type TDD was estimated to be around $3.1 \times 10^8 \text{ cm}^{-2}$, nearly the same as the screw-type TDD, which is consistent with the TEM observations (Figure 2a,b). It is known that edge-type TDs as nonradiative recombination centers (NRCs) are more detrimental to the IQE than screw and mixed type ones.²¹ It should be also noted that the fwhm’s of (20 $\bar{2}$ 1), (20 $\bar{2}$ 3) and (10 $\bar{1}$ m) ($m = 1, 2, 3, 4,$ and 5) DCXRCs for the $\text{Al}_{0.03}\text{Ga}_{0.97}\text{N}$ template were all below 380 arcsec (Figure 3b), further confirming a low density of edge-type TDs.²² The excellent crystalline quality paved the way for realizing electrically injected AlGaIn-based NUV-LDs grown on Si.

The as-grown AlGaIn-based NUV laser epitaxial wafer was subsequently processed into edge-emitting LD devices by using the self-aligned process (see Figure S1 in the Supporting Information). The ridge size was $4 \times 800 \mu\text{m}^2$, and the cavity facets were formed by cleavage, and the front and the rear facets were coated by four and eight pairs of quarter-wave $\text{Ta}_2\text{O}_5/\text{SiO}_2$, respectively, to reduce the mirror loss and the threshold current.

The characteristics of one as-fabricated AlGaIn-based NUV-LD grown on Si under pulsed electrical injection are shown in Figure 4. Figure 4a presents the electroluminescence (EL) spectra of the NUV-LD before cavity facet coating under various injection currents at room temperature. As the injection current was gradually increased from 50 to 500 mA, the peak wavelength was blue-shifted from 392.8 to 389.6 nm due to the screening of the quantum confined Stark effect by the injected carriers. It was noted that due to limited indium in the QWs,

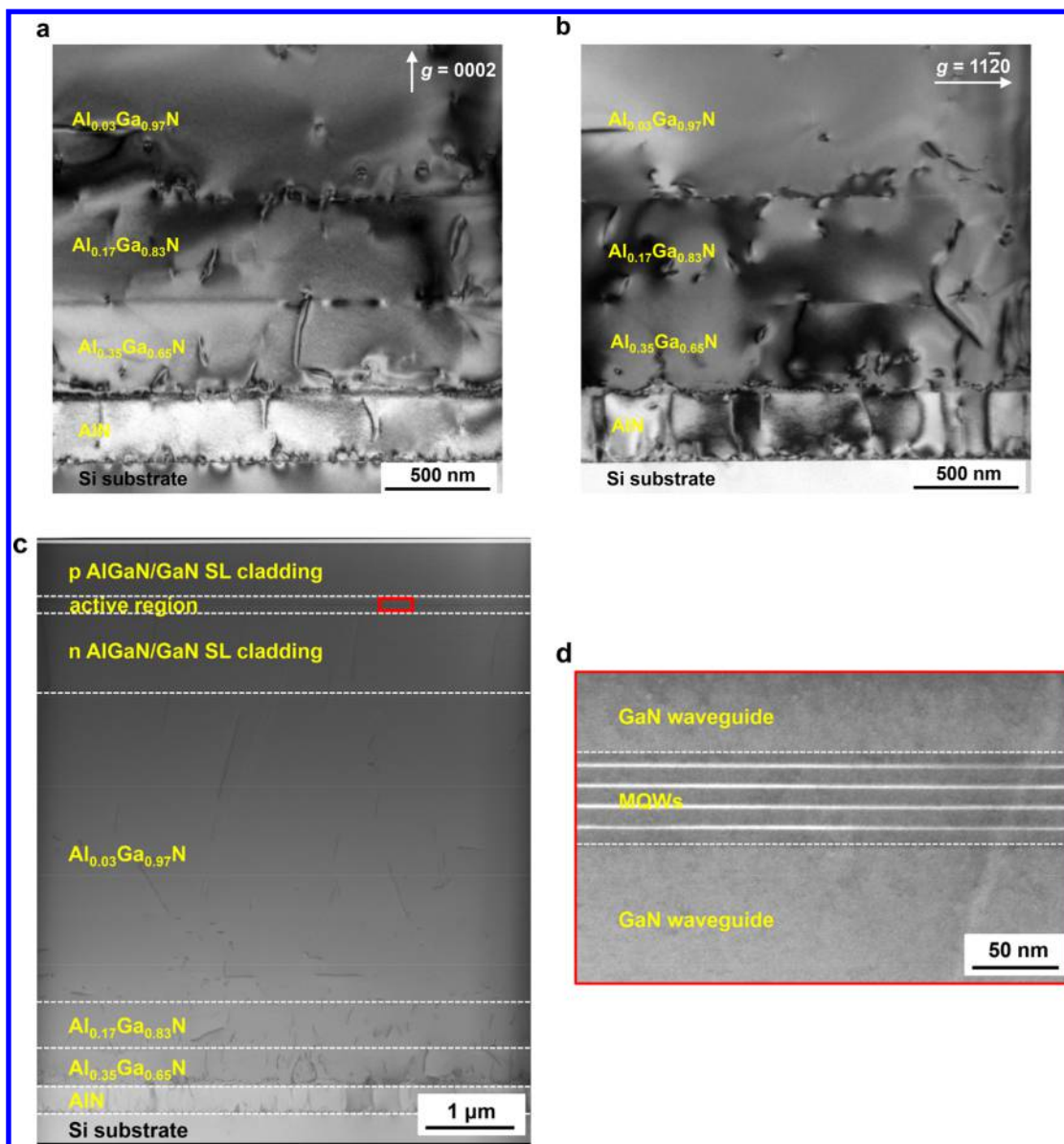


Figure 2. Cross-sectional transmission electron microscopy (TEM) images of an AlGaIn-based NUV laser grown on Si. (a, b) Cross-sectional weak-beam bright-field TEM images of the AlN/AlGaIn multilayer buffer grown on Si obtained with diffraction vectors $g = 0002$ (a) and $g = 11\bar{2}0$ (b) revealing TDs with screw and edge components, respectively. (c) Cross-sectional high-angle annular dark-field scanning TEM image of an AlGaIn-based NUV laser structure grown on Si. The thickness of the whole epitaxial structure was $6.5 \mu\text{m}$. (d) Enlarged image of the $\text{In}_{0.05}\text{Ga}_{0.95}\text{N}/\text{Al}_{0.1}\text{Ga}_{0.9}\text{N}$ NUV QW active region marked with red rectangle in (c).

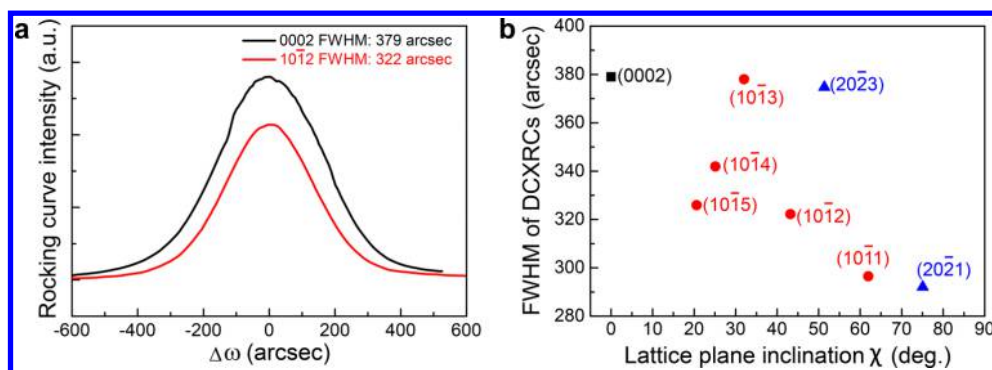


Figure 3. (a) DCXRCs around (0002) and $(10\bar{1}2)$ planes of the $\text{Al}_{0.03}\text{Ga}_{0.97}\text{N}$ template in the AlGaIn-based NUV laser structure grown on Si, and (b) fwhm's of DCXRCs as a function of the lattice plane inclination angle of the $\text{Al}_{0.03}\text{Ga}_{0.97}\text{N}$ template in the NUV laser structure grown on Si.

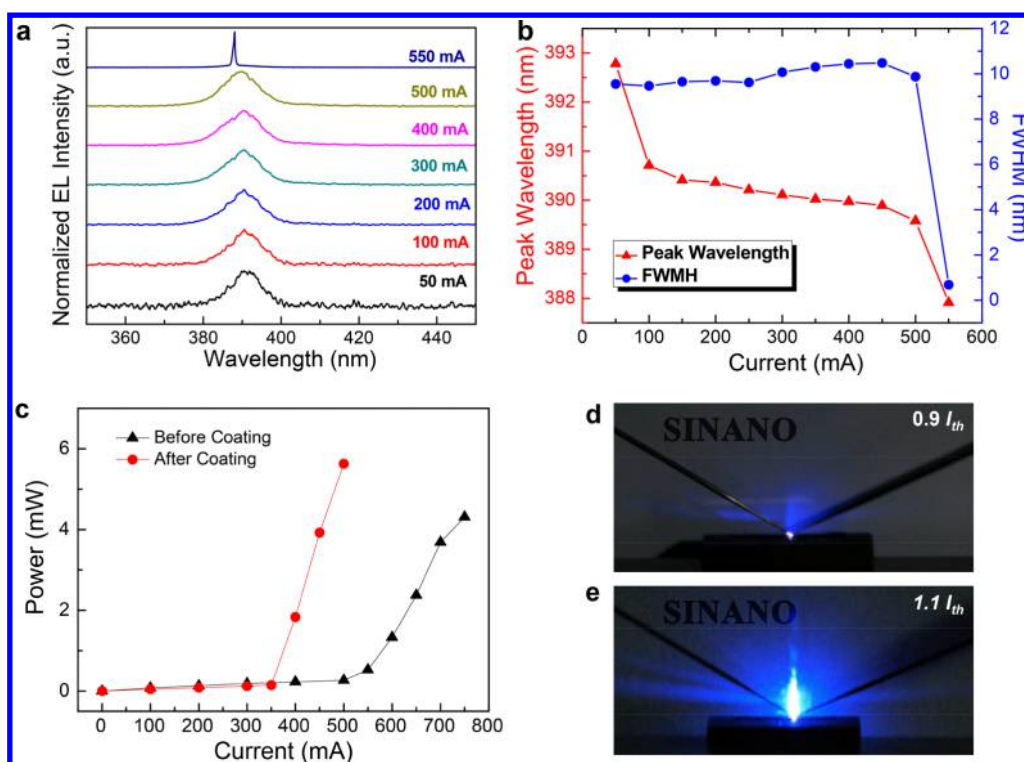


Figure 4. EL characteristics of an as-fabricated AlGaIn-based NUV-LD grown on Si at room temperature. (a) EL spectra of an as-fabricated AlGaIn-based NUV-LD grown on Si before the cavity facet coating measured under various pulsed currents, and the spectral resolution was 0.1 nm. (b) Peak wavelength and fwhm of the EL spectra of the LD before coating as a function of the pulsed injection current. (c) EL light output powers of the LD before and after the cavity facet coating as a function of the pulsed injection current. (d, e) Far-field patterns observed below ($0.9 I_{th}$) (d) and above the threshold current ($1.1 I_{th}$) (e) by setting a sheet of white copying paper in front of the front facet of the NUV-LD under pulsed currents (the pulse width was 400 ns, and the repetition rate 10 kHz) at room temperature, and a blue fluorescence formed when the NUV light illuminated the white copying paper.

the polarization field in the QWs was reduced, and hence, the blue-shift value of the peak wavelength was quite small,²³ as compared with the visible LDs grown on Si. After that, the EL spectra quickly narrowed down and the fwhm of the lasing spectrum was only 0.68 nm (Figure 4b). Figure 4c shows the EL light output power of the NUV-LD as a function of the injection current. The plots of light output versus injection current of the NUV-LD before and after the cavity facet coating exhibit a clear turning point at 550 and 350 mA, respectively, which correspond to a threshold current density of 17.2 and 10.9 kA/cm², respectively. Figure 4d,e shows the far-field patterns of the NUV-LD after the cavity facet coating when the injection current was below and above the threshold current (I_{th}), respectively. All of the above observations are clear signatures of electrically injected lasing at room temperature. The statistical results regarding the threshold current distribution of the as-fabricated AlGaIn-based NUV-LDs grown on Si (see Figure S2 in the Supporting Information) indicate a decent yield and reproducibility for the first demonstration.

As compared with the reported value (~ 3 kA/cm²) of NUV-LD grown on high quality GaN substrates (TDD $\sim 10^6$ cm⁻²) by epitaxial lateral overgrowth (ELOG),⁵ the threshold current density of the as-fabricated AlGaIn-based NUV-LD grown on Si was relatively high, which caused a limited lifetime (~ 1.5 h) under a pulsed injection current of 450 mA (pulse width of 400 ns and a repetition rate of 10 kHz) at room temperature. The relatively high threshold current of the as-fabricated AlGaIn-based NUV-LD grown on Si was related to the relatively high

TDD of $\sim 6 \times 10^8$ cm⁻² (as compared with the homoepitaxial devices),^{5,24} imperfect active region, and point defects. The TDs acting as NRCs caused a substantial portion of the injected carriers to recombine nonradiatively into heat, and it would not only reduce the IQE, but also elevate the junction temperature, which resulted in a significant increase in the threshold current.²⁴ Moreover, previous reports showed that with a reduced indium content, fewer localization states exist in the In_{0.05}Ga_{0.95}N/Al_{0.1}Ga_{0.9}N NUV QWs, and the IQE of the device is much more sensitive to the TDD. Furthermore, thanks to the weakened polarization field in the NUV In_{0.05}Ga_{0.95}N QWs, wider QWs are often used to enhance the optical confinement in AlGaIn-based NUV-LD.⁵ In addition, point defects may also lower the IQE of the LD active region,²⁵ especially in UV QWs.

Previous reports showed that the lifetime of III-nitride LD was improved from 1 s to 300 h^{26,27} when the threshold current density reduced from 9 to 4.2 kA/cm², and it could be further increased to over 10000 h when the TDD in the GaN layer is reduced from 10^8 down to 10^6 cm⁻² through ELOG.¹⁴ The TDD of the AlGaIn layer can also be reduced from 10^8 down to 10^6 cm⁻² through ELOG,²⁸ and the point defect density can be reduced by optimizing the growth conditions and controlling the defect quasi Fermi level.²⁹ A study of AlGaIn ELOG on Si, together with a further optimization of the active region, is underway to reduce the threshold current density and, hence, elongate the lifetime of AlGaIn-based NUV-LD grown on Si.

A high-quality NUV laser structure was successfully grown on Si (111) substrate by using a carefully engineered Al-composition step down-graded AlN/AlGaIn multilayer buffer.

The high crystalline quality of $\text{Al}_{0.03}\text{Ga}_{0.97}\text{N}$ template on Si was confirmed by the observation of TD inclination and annihilation in TEM images and the narrow XRCs for various diffraction planes. After device fabrication, a dramatic narrowing of the EL spectral line-width, an elongated far-field pattern, and a clear discontinuity in the slope of light output power plotted as a function of the injection current provide an unambiguous evidence of lasing. This is the first observation of electrically injected lasing in AlGaIn-based NUV-LD grown on Si at room temperature.

METHODS

Fabrication of Samples. The growth of AlGaIn-based NUV laser structure was carried out with a commercially available MOCVD system. Trimethylgallium, trimethylaluminum, trimethylindium, and ammonia were used as precursors for gallium, aluminum, indium, and nitrogen, respectively. Nitrogen and hydrogen were used as the carrier gas. Monosilane and bisethylcyclopentadienylmagnesium were used as n- and p-type dopants, respectively. As shown in Figure 2, a 300 nm thick AlN nucleation layer was deposited on a thermally cleaned Si(111) substrate. Afterward, Al composition step-graded AlGaIn multilayer consisting of a 420 nm thick $\text{Al}_{0.35}\text{Ga}_{0.65}\text{N}$ layer and a 450 nm thick $\text{Al}_{0.17}\text{Ga}_{0.83}\text{N}$ layer were grown prior to the deposition of $\text{Al}_{0.03}\text{Ga}_{0.97}\text{N}$ thick layer to intentionally introduce compressive strain for the compensation of the tensile stress due to the CTE mismatch during cool down. An AlGaIn-based NUV laser structure (Figure 1) was grown on top of a 3.5 μm thick Si-doped $\text{Al}_{0.03}\text{Ga}_{0.97}\text{N}$ layer. The active region was sandwiched by waveguide and cladding layers. The 80 nm thick n-type and 60 nm thick undoped GaN layers acted as the lower and upper waveguide, respectively. The 750 nm thick n-type $\text{Al}_{0.2}\text{Ga}_{0.8}\text{N}/\text{GaN}$ SL layer and 500 nm thick p-type $\text{Al}_{0.2}\text{Ga}_{0.8}\text{N}/\text{GaN}$ SL layer were CLs, which worked with the waveguides for the optical confinement. The active region was consisted of four pairs of 2.5 nm thick undoped $\text{In}_{0.05}\text{Ga}_{0.95}\text{N}$ QWs and 10 nm thick undoped $\text{Al}_{0.1}\text{Ga}_{0.9}\text{N}$ quantum barrier layers. During the $\text{Al}_{0.1}\text{Ga}_{0.9}\text{N}$ quantum barrier growth, the total flow rates of H_2 , N_2 and NH_3 were 5, 110, and 75 slm, respectively. The as-grown AlGaIn-based NUV laser wafer was mirror-like with less than 0.5 mm long microcracks at the wafer edge area. The AlGaIn-based NUV-LD fabrication process details are shown as Figure S1 in Supporting Information.

Characterization of Samples. TEM (Figure 2a,b) and scanning TEM (Figure 2c,d) images were recorded using an FEI Tecnai G2 F20 S-Twin transmission electron microscope operated at 200 kV. High resolution X-ray rocking curve (Figure 3a,b) measurements were performed with a Bruker D8 discover high resolution X-ray diffractometer.

The light output power under pulsed currents (The pulse width was 400 ns, and the repetition rate 10 kHz) was calculated by the average light output power divided by the duty ratio (4%), and the average light output power was measured by a calibrated optical power meter (Thorlabs PM121D) at room temperature. The EL spectra of the AlGaIn-based NUV-LD were measured by a fiber optic spectrometer (IdeaOptics FX4000) under the pulsed current injection with a pulse width of 400 ns and a repetition rate of 10 kHz.

ASSOCIATED CONTENT

Supporting Information

The Supporting Information is available free of charge on the ACS Publications website at DOI: 10.1021/acsphotonics.7b01215.

Figure S1: The fabrication process of the AlGaIn-based near-ultraviolet lasers grown on Si. Figure S2: The threshold current distribution of AlGaIn-based near-ultraviolet laser grown on Si (PDF).

AUTHOR INFORMATION

Corresponding Author

*E-mail: qsun2011@sinano.ac.cn.

ORCID

Meixin Feng: 0000-0002-3206-6990

Qian Sun: 0000-0001-5495-2232

Dabing Li: 0000-0001-5353-1460

Author Contributions

[‡]These authors contributed equally to this work.

Author Contributions

The manuscript was written through contributions of all authors. All authors have given approval to the final version of the manuscript.

Notes

The authors declare no competing financial interest.

ACKNOWLEDGMENTS

The authors are grateful for the financial support from the National Key R&D Program (Grant Nos. 2016YFB0400100 and 2016YFB0400104), the National Natural Science Foundation of China (Grant Nos. 61534007, 61404156, 61522407, 61604168, and 61775230), the Key Frontier Scientific Research Program of the Chinese Academy of Sciences (Grant No. QYZDB-SSW-JSC014), the Science and Technology Service Network Initiative of the Chinese Academy of Sciences, the Key R&D Program of Jiangsu Province (Grant No. BE2017079), the Natural Science Foundation of Jiangsu Province (Grant No. BK20160401), and the China Postdoctoral Science Foundation (Grant No. 2016M591944). This work was also supported by the open fund of the State Key Laboratory of Luminescence and Applications (Grant No. SKLA-2016-01), the open fund of the State Key Laboratory on Integrated Optoelectronics (Grant Nos. IOSKL2016KF04 and IOSKL2016KF07), and the seed fund from SINANO, CAS (Grant No. Y5AAQ51001). We are thankful for the technical support from Nano Fabrication Facility, Platform for Characterization and Test, Nano-X of SINANO, CAS.

REFERENCES

- (1) Yoshida, H.; Yamashita, Y.; Kuwabara, M.; Kan, H. A 342-nm ultraviolet AlGaIn multiple quantum-well laser diode. *Nat. Photonics* **2008**, *2*, 551–554.
- (2) Taketomi, H.; Aoki, Y.; Takagi, Y.; Sugiyama, A.; Kuwabara, M.; Yoshida, H. Over 1W record-peak-power operation of a 338nm AlGaIn multiple-quantum-well laser diode on a GaN substrate. *Jpn. J. Appl. Phys.* **2016**, *55*, 05FJ05.
- (3) Akasaki, I.; Sota, S.; Sakai, H.; Tanaka, T.; Koike, M.; Amano, H. Shortest wavelength semiconductor laser diode. *Electron. Lett.* **1996**, *32*, 1105–1106.
- (4) Yoshida, H.; Yamashita, Y.; Kuwabara, M.; Kan, H. Demonstration of an ultraviolet 336 nm AlGaIn multiple-quantum-well laser diode. *Appl. Phys. Lett.* **2008**, *93*, 241106.

- (5) Masui, S.; Matsuyama, Y.; Yanamoto, T.; Kozaki, T.; Nagahama, S.; Mukai, T. 365nm Ultraviolet Laser Diodes Composed of Quaternary AlInGaN Alloy. *Jpn. J. Appl. Phys.* **2003**, *42*, L1318–L1320.
- (6) Kneissl, M.; Yang, Z.; Teepe, M.; Knollenberg, C.; Schmidt, O.; Kiesel, P.; Johnson, N. M. Ultraviolet semiconductor laser diodes on bulk AlN. *J. Appl. Phys.* **2007**, *101*, 123103.
- (7) Bidnyk, S.; Little, B. D.; Cho, Y. H.; Krasinski, J.; Song, J. J.; Yang, W.; McPherson, S. A. Laser action in GaN pyramids grown on (111) silicon by selective lateral overgrowth. *Appl. Phys. Lett.* **1998**, *73*, 2242–2244.
- (8) Lutsenko, E. V.; Pavlovskii, V. N.; Zubilevich, V. Z.; Stognij, A. I.; Gurskii, A. L.; Hryshanau, V. A.; Shulenkov, A. S.; Yablonskii, G. P.; Schon, O.; Protmann, H.; Lünenbürger, M.; Schineller, B.; Dikme, Y.; Jansen, R. H.; Heuken, M. Growth, stimulated emission, photo- and electroluminescence of InGaN/GaN EL-test heterostructures. *Phys. Status Solidi C* **2003**, *0*, 272–275.
- (9) Shuhaimi, B. A. B. A.; Kawato, H.; Zhu, Y.; Egawa, T. Growth of InGaN-based laser diode structure on silicon (111) substrate. *J. Phys.: Conf. Ser.* **2009**, *152*, 012007.
- (10) Kushimoto, M.; Tanikawa, T.; Honda, Y.; Amano, H. Optically pumped lasing properties of (1–101) InGaN/GaN stripe multi-quantum wells with ridge cavity structure on patterned (001) Si substrates. *Appl. Phys. Express* **2015**, *8*, 022702.
- (11) Sun, Y.; Zhou, K.; Sun, Q.; Liu, J. P.; Feng, M. X.; Li, Z. C.; Zhou, Y.; Zhang, L. Q.; Li, D. Y.; Zhang, S. M.; Ikeda, M.; Liu, S.; Yang, H. Room-temperature continuous-wave electrically injected InGaN-based laser directly grown on Si. *Nat. Photonics* **2016**, *10*, 595–599.
- (12) Li, D. GaN-on-Si laser diode: open up a new era of Si-based optical interconnections. *Sci. Bull.* **2016**, *61*, 1723–1725.
- (13) Hirayama, H.; Maeda, N.; Fujikawa, S.; Toyoda, S.; Kamata, N. Recent progress and future prospects of AlGaIn-based high-efficiency deep-ultraviolet light-emitting diodes. *Appl. Phys. Express* **2014**, *53*, 100209.
- (14) Nakamura, S. The roles of structural imperfections in InGaIn-Based blue light-emitting diodes and laser diodes. *Science* **1998**, *281*, 956–961.
- (15) Amano, H.; Nagamatsu, K.; Takeda, K.; Mori, T.; Tsuzuki, H.; Iwaya, M.; Kamiyama, S.; Akasaki, I. Growth and conductivity control of high quality AlGaIn and its application to high-performance ultraviolet laser diodes. *Proc. SPIE* **2009**, *7216*, 72161B.
- (16) Feezell, D. F.; Schmidt, M. C.; Farrell, R. M.; Kim, K.; Saito, M.; Fujito, K.; Cohen, D. A.; Speck, J. S.; Denbaars, S. P.; Nakamura, S. AlGaIn-Cladding-Free Nonpolar InGaIn/GaN Laser Diodes. *Jpn. J. Appl. Phys.* **2007**, *46*, L284–L286.
- (17) Kim, D. Y.; Park, J. H.; Lee, J. W.; Hwang, S.; Oh, S. J.; Kim, J.; Sone, C.; Schubert, E. F.; Kim, J. K. Overcoming the fundamental light-extraction efficiency limitations of deep ultraviolet light-emitting diodes by utilizing transverse-magnetic-dominant emission. *Light: Sci. Appl.* **2015**, *4*, e263.
- (18) Li, Z.; Liu, L.; Huang, Y.; Sun, Q.; Feng, M.; Zhou, Y.; Zhao, H.; Yang, H. High-power AlGaIn-based near-ultraviolet light-emitting diodes grown on Si(111). *Appl. Phys. Express* **2017**, *10*, 072101.
- (19) Sun, Q.; Yan, W.; Feng, M. X.; Li, Z. C.; Feng, B.; Zhao, H. M.; Yang, H. GaIn-on-Si Blue/White LEDs: Epitaxy, Chip, and Package. *J. Semicond.* **2016**, *37*, 044006.
- (20) Leung, B.; Han, J.; Sun, Q. Strain relaxation and dislocation reduction in AlGaIn step-graded buffer for crack-free GaIn on Si (111). *Phys. Stat. Sol. C* **2014**, *11*, 437–441.
- (21) Chems, D.; Henley, S. J.; Ponce, F. A. Edge and screw dislocations as nonradiative centers in InGaIn/GaN quantum well luminescence. *Appl. Phys. Lett.* **2001**, *78*, 2691–2693.
- (22) Heying, B.; Wu, X. H.; Keller, S.; Li, Y.; Kopolnek, D.; Keller, B. P.; DenBaars, S. P.; Speck, J. S. Role of threading dislocation structure on the x-ray diffraction peak widths in epitaxial GaIn films. *Appl. Phys. Lett.* **1996**, *68*, 643–645.
- (23) Bernardini, F.; Vincenzo, F.; Vanderbilt, D. Spontaneous polarization and piezoelectric constants of III–V nitrides. *Phys. Rev. B: Condens. Matter Mater. Phys.* **1997**, *56*, 10024–10027.
- (24) Tomiya, S.; Hino, T.; Goto, S.; Takeya, M.; Ikeda, M. Dislocation related issues in the degradation of GaIn-based laser diodes. *IEEE J. Sel. Top. Quantum Electron.* **2004**, *10*, 1277–1286.
- (25) Chichibu, S. F.; Onuma, T.; Kubota, M.; Uedono, A.; Sota, T.; Tsukazaki, A.; Ohtomo, A.; Kawasaki, M. Improvements in quantum efficiency of excitonic emissions in ZnO epilayers by the elimination of point defects. *J. Appl. Phys.* **2006**, *99*, 093505.
- (26) Nakamura, S.; Senoh, M.; Nagahama, S.; Iwasa, N.; Yamada, T.; Matsushita, T.; Sugimoto, Y.; Kiyoku, H. Room-temperature continuous-wave operation of InGaIn multi-quantum-well structure laser diodes. *Appl. Phys. Lett.* **1996**, *69*, 4056–4058.
- (27) Nakamura, S.; Senoh, M.; Nagahama, S.; Iwasa, N.; Yamada, T.; Matsushita, T.; Sugimoto, Y.; Kiyoku, H. High-power, long-lifetime InGaIn multi-quantum-well structure laser diodes. *Jpn. J. Appl. Phys.* **1997**, *36*, L1059–L1061.
- (28) Iida, K.; Kawashima, T.; Miyazaki, A.; Kasugai, H.; Mishima, S.; Honshio, A.; Miyake, Y.; Iwaya, M.; Kamiyama, S.; Amano, H.; Akasaki, I. 350.9nm UV Laser Diode Grown on Low-Dislocation-Density AlGaIn. *Jpn. J. Appl. Phys.* **2004**, *43*, L499–L500.
- (29) Reddy, P.; Hoffmann, M. P.; Kaess, F.; Bryan, Z.; Bryan, I.; Bobea, M.; Klump, A.; Tweedie, J.; Kirste, R.; Mita, S.; Gerhold, M.; Collazo, R.; Sitar, Z. Point defect reduction in wide bandgap semiconductors by defect quasi Fermi level control. *J. Appl. Phys.* **2016**, *120*, 185704.